AND8222/D

Predicting the Effect of Circuit Boards on Semiconductor Package Thermal Performance

Prepared by: Roger Paul Stout, PE
ON Semiconductor

ON Semiconductor®

http://onsemi.com

APPLICATION NOTE

Abstract

In some situations, a circuit board may be approximated by varying regions of roughly axisymmetric geometry, and a cascaded two−port model may be easily constructed and solved analytically. Each axisymmetric segment of the model is a two−port (in thermal terms, a circular fin lacking the traditional adiabatic boundary condition at the outer radius), hence an arbitrarily complex (axisymmetric) board model is represented by a cascaded two−port network. The overall network is driven by a heat source at its inner radius, and some outer radius boundary condition; the two−port concept naturally separates the interior conduction and surface convection properties from the temperature and heat flux boundary conditions. Using this scheme, temperature and heat flow may be easily determined at every position within the model, thus providing necessary information on the interactions between locations within the model − permitting yet more complex analyses of a circuit board as a multiple heat source system. Application of the axisymmetric two−port method is made to thermal characterization of semiconductor devices, including the relationship between so called "min pad" and "1−inch pad" device characteristics. The model is also compared to other experimental data, where the "best fit" of the model parameters shows a reasonable correlation with the expected physical values of the experiment.

Key Words

thermal analytical model axisymmetric two−port

Glossary of Symbols

A	cross−section conduction area (m^2)
A, B, C, D	two−port transmission parameters
a, b	general purpose constants
G	thermal conductance ($W \cdot C^{-1}$)
h	film coefficient ($W \cdot C^{-1} m^{-2}$)
$I_p(z)$	modified Bessel function of the first kind
$K_p(z)$	modified Bessel function of the second kind
k	fin (board) conductivity ($W \cdot C^{-1} m^{-1}$)
m	system parameter (m^{-1})
q	heat flow (W)
Q	total device power dissipation (W)
r	radial coordinate (m)
T	temperature variable (C)
T_∞	bulk fluid temperature (C)
T	two−port transmission matrix
t	fin (board) thickness (m)
z	dimensionless radius

Greek Symbols

Ψ	temperature rise/device power dissipation ($C \cdot W^{-1}$)
θ	temperature rise above bulk fluid temperature (C)

Subscripts and Superscripts

i, j, k, o	board region or boundary designations
b, s, e	beginning, spreader, ending boundary designations
p	order of Bessel function

INTRODUCTION

In the semiconductor package thermal characterization business, it is ultimately desirable to accurately describe device performance in an actual application environment. Obviously this performance is the result of a combined package and system, thus one must know both the package and the system characteristics in order to answer the question. The reality is that the interaction between a package and its environment may be quite complex (e.g., multiple and significant parallel heat paths, and temperature dependent behavior). Nonetheless it is convenient, and in many cases adequate for first−order estimates, to consider that a uniquely identifiable and clean boundary separates the package from its environment (which, for the purposes of this discussion, will be simply a "board"). From the package's perspective, the board simply absorbs heat (power), and, all else being equal, responds by attaining a predictable temperature at the package/board interface.

From the board's perspective, the package is simply a heat source, the location of the package defining a "boundary" of the board. The power injected into the board by the package constitutes a boundary condition of the model, and the local temperature varies in response. Ambient provides a second boundary condition for the board. It is a fixed temperature, and the ultimate sink for all the power injected by the package. So for a board with a single package present, there is an input heat source and associated temperature, and an output heat "sink" with a second associated temperature.

A circuit board may therefore be thought of as a thermal resistance between the package and ambient, even though it is distinguished from a traditional thermal resistance in that it "leaks" heat to convention as it flows from the input end to the output end.

Two−Ports

In the electrical realm, the external view of a network generally consists of terminals, often grouped in pairs. A terminal pair, or port, is then represented as having a potential, or voltage, between the two terminals of the port, and a current flow into (and return from) the network at that port. A network may have any number of ports, but if it may be described using two ports, it is classified as a two−port network, or more simply, a "two−port." The literature is rich in theory and applications of electrical two−ports, in particular, passive, linear systems which will be the focus here (1,2).

Using the conventional thermal−electrical analogy, thermal "potential" is temperature, corresponding to voltage; thermal "flow" is power, corresponding to current. A circuit board having a single point heat input, and a single output boundary condition, is, therefore, a thermal two−port.

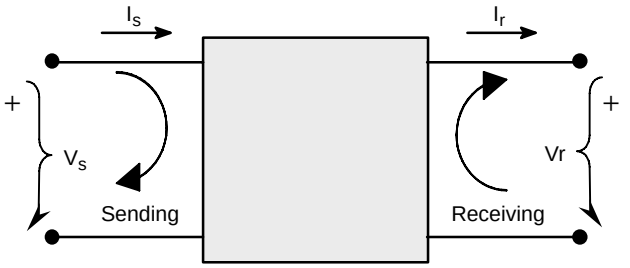

Figure 1. Electrical Two−Port

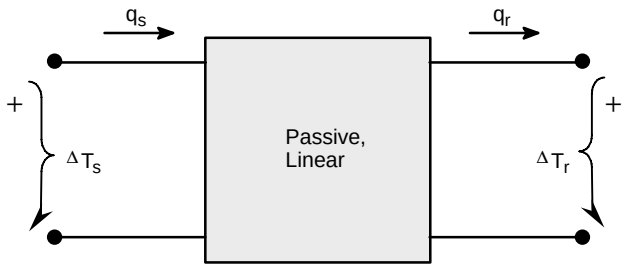

Figure 2. Thermal Two−Port

Note that two−port theory does not require that flow out the receiving port equals flow into the sending port. Rather, the model describes an overall relationship between the four quantities associated with the two ports, as shown in Equation 1, and represents the internal system by way of the *transmission parameters* of the two−port: A, B, C, and D.

$$\begin{Bmatrix} \Delta T_s \\ q_s \end{Bmatrix} = \begin{bmatrix} A & B \\ C & D \end{bmatrix} \begin{Bmatrix} \Delta T_r \\ q_r \end{Bmatrix} \quad \text{(eq. 1)}$$

The transmission matrix, then, is defined as:

$$\mathbf{T} = \begin{bmatrix} A & B \\ C & D \end{bmatrix} \quad \text{(eq. 2)}$$

The nature of a two−port is to permit a continuum of boundary conditions at each port, trading off potential for flow, and vice versa. Further, the trade off at one port influences the conditions at the other port. For instance, an adiabatic boundary at the receiving port ($q_r = 0$) translates into particular expressions for both potential and flow at the sending end, purely in terms of the potential at the receiving end:

$$\begin{aligned} \Delta T_s &= A \cdot \Delta T_r \\ q_s &= C \cdot \Delta T_r \end{aligned} \quad \text{(eq. 3)}$$

A zero potential at the receiver ($\Delta T_r = 0$) results in different relationships:

$$\begin{aligned} \Delta T_s &= B \cdot q_r \\ q_s &= D \cdot q_r \end{aligned} \quad \text{(eq. 4)}$$

Alternatively, values may be specified at the sender's port, and corresponding expressions derived for the receiver, by inverting Equation 1:

$$\begin{Bmatrix} \Delta T_r \\ q_r \end{Bmatrix} = \begin{bmatrix} A & B \\ C & D \end{bmatrix}^{-1} \begin{Bmatrix} \Delta T_s \\ q_s \end{Bmatrix} \quad \text{(eq. 5)}$$

It turns out that for a properly formulated two−port (1,2), the determinant of the transmission matrix will be unity (which also implies that the four transmission parameters are not completely independent), i.e.:

$$\det \begin{bmatrix} A & B \\ C & D \end{bmatrix} = 1 \quad \text{or} \quad AD-BC = 1 \quad \text{(eq. 6)}$$

Equation 5 becomes:

$$\begin{Bmatrix} \Delta T_r \\ q_r \end{Bmatrix} = \frac{1}{AD-BC} \begin{bmatrix} D & -B \\ -C & A \end{bmatrix} \begin{Bmatrix} \Delta T_s \\ q_s \end{Bmatrix}$$

hence: (eq. 7)

$$\begin{Bmatrix} \Delta T_r \\ q_r \end{Bmatrix} = \begin{bmatrix} D & -B \\ -C & A \end{bmatrix} \begin{Bmatrix} \Delta T_s \\ q_s \end{Bmatrix}$$

Simple Boards as Two−Ports

It may now be seen that a simple circuit board, a “leaky” thermal resistance, having a single package as a heat source and a single ambient thermal ground, fits the two−port model. The sending port is the package (injecting heat into the system), and the receiving port represents the thermally distant environment, perhaps the edges of the board or even farther away. The driving potential at the sending port is the temperature differential between the package/board interface and some convenient reference temperature. The potential at the receiving port is a similar temperature differential between some location in the thermal system being modeled, and some other convenient reference temperature.

In many semiconductor applications, it is sensible to reference all temperatures to some common ambient. In particular, both the sending potential (the package/board interface temperature), and the receiving potential (the board perimeter temperature), should be referenced to ambient. Indeed, it will be seen that this is a necessary step in creating a thermal two−port representing a circuit board. It is *not* necessary that the receiving temperature itself *be* ambient; if this happens to be so, it is the special case where the receiving potential is zero (analogous to the short−circuit behavior of an electrical two−port).

What then should be the receiving port, that is, what temperature and location in a circuit board thermal model should be selected as the receiving port? To make sense mathematically, the temperature must be an isotherm of the system. That is to say, since a single scalar value is being used in the model to represent the temperature at some location in the system, it simultaneously represents *all* the points in the system sharing that same temperature. To make sense physically, the requirement is to identify an isotherm that remains an isotherm over the operating range of interest in the system (which is not to say that the temperature of the isotherm is constant, but rather that its shape remain fixed.) In real world systems, we may have to compromise. Whatever isotherm is chosen as the receiving port will influence the particular transmission parameters for that model. Our goal should be to choose a useful one.

Axisymmetric Board

Consider the very simple model of a circuit board shown in Figure 3. What is particularly helpful about the axisymmetric model is that by definition the outer edge of the board will be an isotherm, hence an acceptable choice as the receiving port of the two−port. In this model, there is an axisymmetric heat source at the inner radius (the package), and an exterior circular perimeter of the board at which we will specify both a temperature rise above ambient and possibly a heat flow from the edge. Between the inner and outer radii, board properties are uniform, and heat is lost continuously to convection, characterized by a constant film coefficient. Note that if the heat loss at the outer radius is zero, we have a conventional circular fin, whose solution may be found in any number of references (3,4). We are interested here, however, in the more general case where the outer edge is neither adiabatic nor a fixed temperature, i.e., it is a thermal “port.”

The governing equation for this system (5,6) is:

$$\frac{d^2T}{dr^2} + \frac{1}{r}\frac{dT}{dr} - \frac{2h}{kt}(T - T_\infty) = 0 \qquad \text{(eq. 8)}$$

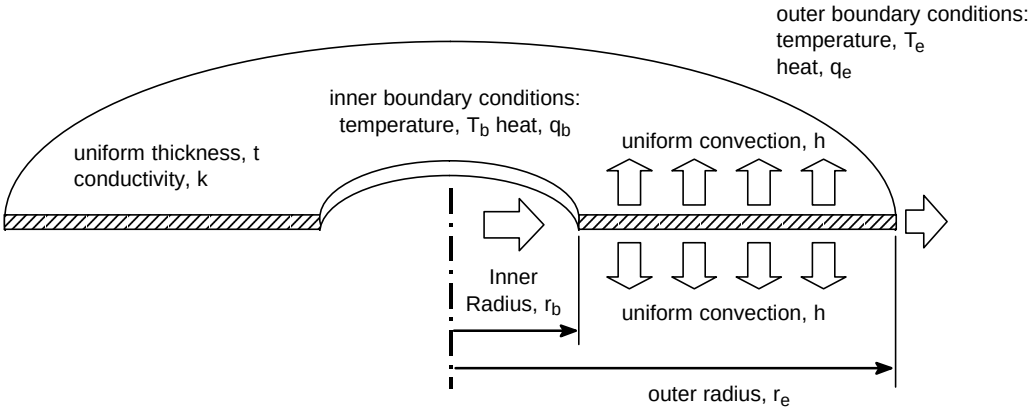

Figure 3. Basic Problem Geometry

With the following changes of variables,

$$\theta = T - T_\infty \quad \text{(eq. 9)}$$

$$m = \sqrt{\frac{2h}{kt}} \quad \text{(eq. 10)}$$

$$z = mr \quad \text{(eq. 11)}$$

Equation 8 becomes:

$$\frac{d^2\theta}{dz^2} + \frac{1}{z}\frac{d\theta}{dz} - \theta = 0 \quad \text{(eq. 12)}$$

Note that with this definition of θ, all temperatures in the model (throughout the domain, inclusive of the two boundaries) become thermal potentials, now referenced to the common ambient. Being a second order, homogeneous ordinary differential equation, the general solution of Equation 12 may be written (7) as follows:

$$\theta = aI_0(z) + bK_0(z) \quad \text{(eq. 13)}$$

where a and b are arbitrary constants, and $I_0(z)$ and $K_0(z)$ are the *modified Bessel functions* of the first and second kinds, respectively. (Additional detail may be found in the Appendix.) Since we also are interested in flow related boundary conditions for the two−port, we must utilize the basic Fourier heat conduction equation, that is:

$$q = -kA(r)\frac{dT}{dr} \quad \text{(eq. 14)}$$

which relates local temperature gradients (changes in potential) to local heat flow. Equation 14 was in fact central to the derivation of the original governing Equation 8. Again using the change of variables from r into z, we have:

$$\begin{aligned} q &= -k \cdot t \cdot 2\pi r \cdot \frac{d\theta}{dz}\frac{dz}{dr} \\ &= -2\pi ktmr\theta' \\ &= -2\pi ktz\theta' \end{aligned} \quad \text{(eq. 15)}$$

Equation 15 thus leads to a second expression in the two arbitrary constants (refer again to the Appendix for additional detail on the Bessel functions), specifically:

$$q = -2\pi ktz[aI_1(z) - bK_1(z)] \quad \text{(eq. 16)}$$

Axisymmetric Board as a Two−Port

We may now put the axisymmetric board solution into the form of a two−port. Observe that together, Equations 13 and 16 constitute a system of two equations in the two unknowns a and b, given appropriate boundary values for the potential and flow.

In matrix form, these equations become:

$$\begin{Bmatrix} \theta_i \\ q_i \end{Bmatrix} = \begin{pmatrix} I_0(z_i) & K_0(z_i) \\ -G_iI_1(z_i) & G_iK_1(z_i) \end{pmatrix} \begin{Bmatrix} a \\ b \end{Bmatrix} \quad \text{(eq. 17)}$$

where:

$$G_i = 2\pi ktz_i \quad \text{(eq. 18)}$$

We thus can solve for a and b given a potential and flow at any position within the domain. For instance, if specified at some z_i, then:

$$\begin{Bmatrix} a \\ b \end{Bmatrix} = \begin{pmatrix} I_0(z_i) & K_0(z_i) \\ -G_iI_1(z_i) & G_iK_1(z_i) \end{pmatrix}^{-1} \begin{Bmatrix} \theta_i \\ q_i \end{Bmatrix} \quad \text{(eq. 19)}$$

Now if the domain is defined over a range from z_1 to z_2, inclusive, then Equation 19 is true for the two endpoints z_1 and z_2, that is:

$$\begin{Bmatrix} a \\ b \end{Bmatrix} = \begin{pmatrix} I_0(z_1) & K_0(z_1) \\ -G_iI_1(z_1) & G_iK_1(z_1) \end{pmatrix}^{-1} \begin{Bmatrix} \theta_1 \\ q_1 \end{Bmatrix} \quad \text{(eq. 20)}$$

and also:

$$\begin{Bmatrix} a \\ b \end{Bmatrix} = \begin{pmatrix} I_0(z_2) & K_0(z_2) \\ -G_iI_1(z_2) & G_iK_1(z_2) \end{pmatrix}^{-1} \begin{Bmatrix} \theta_2 \\ q_2 \end{Bmatrix} \quad \text{(eq. 21)}$$

We can therefore eliminate a and b between Equations 20 and 21, leaving an expression for the boundary conditions at one end of the domain in terms of those at the other end of the domain:

$$\begin{Bmatrix} \theta_1 \\ q_1 \end{Bmatrix} = \begin{pmatrix} I_0(z_1) & K_0(z_1) \\ -G_iI_1(z_1) & G_iK_1(z_1) \end{pmatrix} \begin{pmatrix} I_0(z_2) & K_0(z_2) \\ -G_iI_1(z_2) & G_iK_1(z_2) \end{pmatrix}^{-1} \begin{Bmatrix} \theta_2 \\ q_2 \end{Bmatrix} \quad \text{(eq. 22)}$$

Recall now Equation 1:

$$\begin{Bmatrix} \Delta T_s \\ q_s \end{Bmatrix} = \begin{bmatrix} A & B \\ C & D \end{bmatrix} \begin{Bmatrix} \Delta T_r \\ q_r \end{Bmatrix} \quad \text{(eq. 23)}$$

It should be evident that Equation 22 is the two−port representation of the axisymmetric board model in accordance with Equation 1. Finally, the transmission matrix for the two−port is the following two by two matrix product:

$$\mathbf{T}_{ij} = \begin{pmatrix} I_0(z_i) & K_0(z_i) \\ -G_iI_1(z_i) & G_iK_1(z_i) \end{pmatrix} \begin{pmatrix} I_0(z_j) & K_0(z_j) \\ -G_jI_1(z_j) & G_jK_1(z_j) \end{pmatrix}^{-1} \quad \text{(eq. 24)}$$

or

$$\mathbf{T}_{ij} = \begin{bmatrix} A_{ij} & B_{ij} \\ C_{ij} & D_{ij} \end{bmatrix} \quad \text{(eq. 25)}$$

where the subscript pairs indicate that it applies over the domain spanning boundaries i and j. Certainly Equation 24 could be expanded to provide expressions for each of the four transmission parameters explicit in Equation 25 – see the Appendix − but there is no particular benefit in doing so. Indeed, presuming that a computerized tool of some sort will be used to perform actual calculations, there is less opportunity for error in implementing the form of Equation 24 directly, given its symmetry and relative clarity. (Refer again to the Appendix). Observe, also, that the symmetry of Equation 24 demonstrates that simply exchanging boundary subscripts corresponds exactly to obtaining the reverse transmission matrix, i.e.:

$$\mathbf{T}_{ji} = \mathbf{T}_{ij}^{-1} \quad \text{(eq. 26)}$$

In other words, so long as our bookkeeping is consistent, we can build our transmission matrices symbolically in whichever “orientation” is desired (small radius to large, or vice versa). The sending port need not be the heat source at all, unless this is convenient for the problem at hand.

Single−Zone Thermal Test Board

The Appendix shows how the axisymmetric transmission matrix of Equation 24 may be used to derive the following expression for the temperature distribution in a circular board with an adiabatic edge. This may also be found under the guise of a “circular fin” in references such as (3) and (7). In Equation 27, the b subscript represents the base of the fin (the sending port), and the e subscript the adiabatic outer radius of the fin (the receiving port):

$$\frac{T-T_\infty}{T_b-T_\infty} = \frac{K_1(mr_e)I_0(mr) + I_1(mr_e)K_0(mr)}{K_1(mr_e)I_0(mr_b) + I_1(mr_e)K_0(mr_b)} \quad \text{(eq. 27)}$$

When a real thermal test board is considered, none of the “constants” may actually be known accurately, especially considering that we’re using this axisymmetric model to approximate a rectilinear geometry (and even then, rectangular circuit boards are generally far from uniform in material properties, thanks to buried irregular metal planes and actual circuit traces everywhere). Thus, if temperatures are measured at known distances from a heat source, the best choices for T_b, r_b, r_e, and m may be better left as a statistical “best fit” problem. Our main interest here is whether or not the temperature profile derived for a uniform axisymmetric circuit board, bears any resemblance at all to a real temperature profile of a real board. If so, we can learn much about the trade−offs of board properties (size, conductivity, convection coefficient) holding the package itself as a constant.

For this comparison, it is useful to rephrase Equation 27 in terms of our usual “normalized” temperatures where everything is related to the total power dissipation of the heat source in question, Q (that is, the heat input at the inside radius r_b), and the bulk convecting fluid temperature T_∞. For simplicity in the best fit process, we have chosen the following form of the solution (see Appendix):

$$\frac{T-T_\infty}{Q} = c\left[I_0(mr) + \frac{I_1(mr_e)}{K_1(mr_e)}K_0(mr)\right] \quad \text{(eq. 28)}$$

where c, m, and r_e are the independent fit parameters. (Following JEDEC terminology (8−10), this quantity would be known as Ψ_{BA}, or psi−BA, the board−to−ambient temperature difference normalized by package power dissipation.)

Figure 4 illustrates an actual thermal test situation where two components of interest were mounted on a customer’s board, providing an excellent opportunity to compare the analytical board model Equation 28 to a real application. This circuit board had a fairly continuous embedded power plane, so its thermal conductivity would be expected to be reasonably uniform over a large area. Each device (a two−channel TMOS driver) could be heated at either end, and several thermocouples were placed on the board as indicated in the figure. (Not shown is a TC on the back side of the board.) Between the four heat sources and eight TC’s, approximately 30 different samples of temperature rise vs. distance were available.

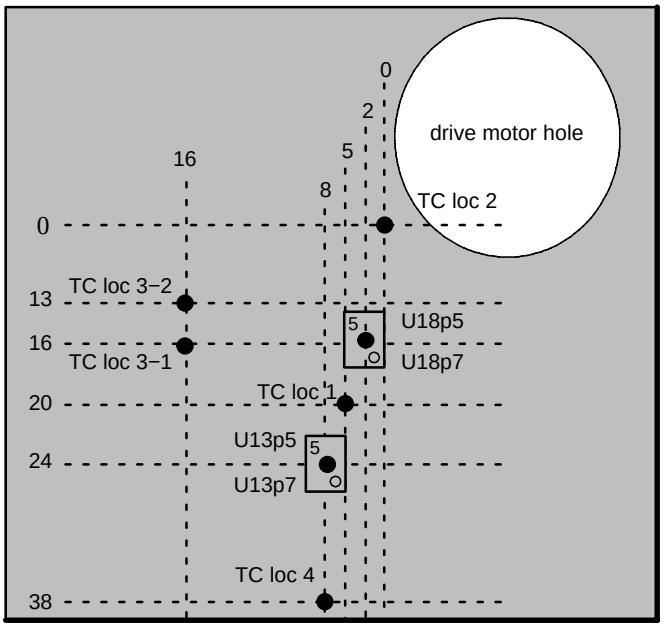

Figure 4. Board Diagram of Heat Sources and TC Locations

Two different test configurations were measured. Figure 5 shows the results (normalized data vs. the best−fit board models) where both sides of the test board were exposed to free convection conditions. Figure 6 shows the results where only one side was exposed to convection, and the other blocked from convection with a thick layer of low density insulating foam. The best fit parameters could, if desired, be compared with the theoretical values based on the known properties, or conversely, used to estimate what the material and convection properties must be in order to give those parameter values. The main point to be made here is that this “physics based” axisymmetric model, of board temperature variation with distance from heat source, is clearly a very reasonable approach, even for a real application board with rectangular geometry and other non−ideal attributes.

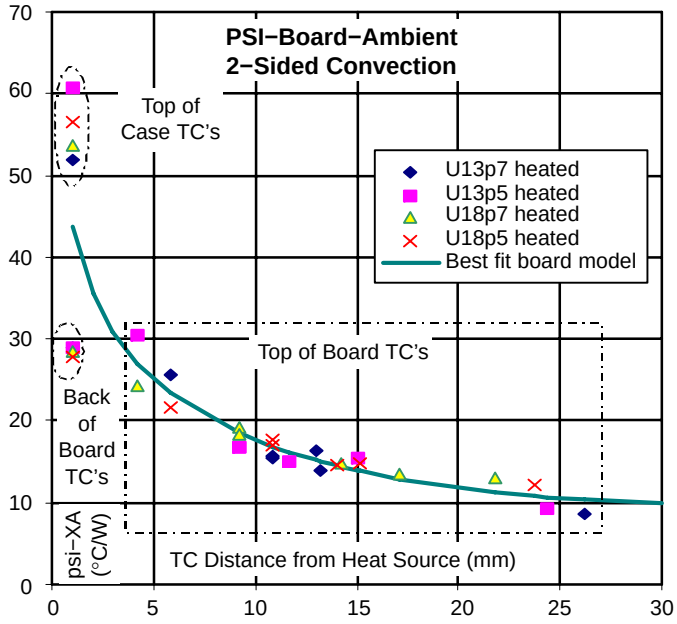

Figure 5. Closed−Form Best Fit to 2−Sides Convection Data

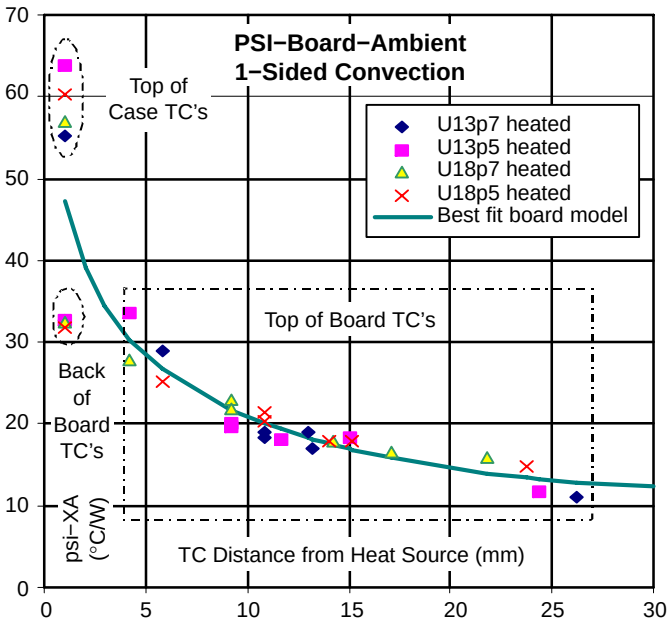

Figure 6. Closed−Form Best Fit to 1−Side Convection Data

Multiple−Zone Two−Port Board Model

In the semiconductor component manufacturer's thermal characterization business, commonly encountered board designs are the so−called "1−inch pad" test boards (Figure 7).

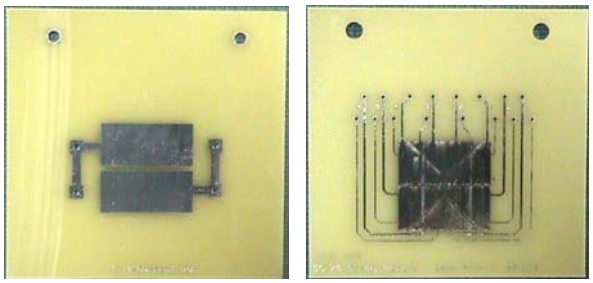

Figure 7. 1−Inch Pad Test Boards for 2 and 8−Lead Devices

In these designs, a plated−on copper heat spreader surrounds the immediate vicinity of the test device (generally mounted at the center of the heat spreader). The spreader is itself much smaller than the entire test board. Thus the effective thermal conductivity of the board changes radically from an inner zone to an outer zone. Even with the simplifying assumption of axisymmetry, the "brute force" approach to this problem would be to return to the original governing Equation 8, solve it for two separate zones with continuity conditions at their interface, and apply appropriate boundary conditions at the overall inner and outer radii.

The two−port approach is far more elegant. Buried within the transmission parameters of Equation 23 is all the internal behavior of the domain, including the details of the physics, the geometry, and even the nature of the coordinate system. The ports are the boundary conditions. When two−ports are cascaded, each interface is by definition an application of continuity (equal potential, conservation of flow).

For instance, to represent the 1−inch pad test board, we may most simply write just two transmission matrices, multiply them through, and apply the desired overall boundary conditions:

$$\begin{Bmatrix} \theta_b \\ q_b \end{Bmatrix} = \mathbf{T}_{bs} \cdot \mathbf{T}_{se} \cdot \begin{Bmatrix} \theta_e \\ q_e \end{Bmatrix} \qquad \text{(eq. 29)}$$

where here we have labeled the boundary of the spreader area as interface s, so the inner domain $(b-s)$ is covered by the 1−inch heat spreader, and the outer domain $(s-e)$ is plain circuit board material. (Using the axisymmetric formulation, we assume there to be a circular isotherm separating the plated zone from the bare zone. A sensible choice for the radius of boundary s is that which gives the same area as the square heat spreader.) We may apply a different film coefficient to each zone, if desired, but at the very least, the effective conductivity of the board will be different in the two regions due to the plating on the inner region.

If we don't care about the temperatures anywhere in between the base and the end, Equation 29 is all there is to it. For example, we can now easily explore the first of two commonly asked questions in semiconductor packaging, namely what is the difference in thermal performance on a "min pad" vs. a 1−inch pad for a particular package? (A min−pad board has no metal except the minimum traces and pads necessary to mount the device and access it electrically.) Intuitively, we know that the min−pad performance is a strong function of the size of the package, and that 1−inch pad performance is much better than min−pad performance. Equation 29 gives us a simple, yet physics−based answer to this question. Note also that if both inner and outer regions are given the same (unplated) board material properties, Equation 29 applies equally well for the min−pad board.

Let us rephrase Equation 29 in terms more specific to our immediate interest:

$$\begin{Bmatrix} T_b - T_\infty \\ Q \end{Bmatrix} = \mathbf{T}_{bs} \cdot \mathbf{T}_{se} \cdot \begin{Bmatrix} T_e - T_\infty \\ 0 \end{Bmatrix} \qquad \text{(eq. 30)}$$

As before, T_∞ is the bulk fluid temperature (i.e., ambient). T_b is the board temperature, found at the inner domain boundary radius r_b (that is, the inner boundary of the 1−inch copper plated region). Q is the total package power dissipation, which is input at r_b.

The inner radius itself, r_b, represents the package "size". To get the most use out of the results, ultimately we will want to correlate specific package geometries of interest to this "generic" package size parameter. For example, in a standard dual inline type package, r_b might best be represented as half the distance from the leads on one side of the package to the leads on the other side of the package; whereas for a soldered heatsink type device, the best choice might be the radius giving the same area as the actual heatsink. In any event, r_b is a fundamental variable in this analysis, implicit in $\mathbf{T}_{bs}$.

Finally, T_e is the board temperature at the outer radius of the plain circuit board material domain, r_e. (To be consistent, its value will be the radius that gives the same area as the actual total area of the test board.) Though we don't as yet have a value for T_e, we have assumed in Equation 30 that the exterior radius of the test board is adiabatic (meaning the outer radius heat flow is expressly zero).

Introducing our subscript notation to indicate the domain of application:

$$\begin{bmatrix} A_{be} & B_{be} \\ C_{be} & D_{be} \end{bmatrix} = \mathbf{T}_{bs} \cdot \mathbf{T}_{se} \qquad \text{(eq. 31)}$$

Using this, Equation 30 becomes:

$$\begin{Bmatrix} T_b - T_\infty \\ Q \end{Bmatrix} = \begin{bmatrix} A_{be} & B_{be} \\ C_{be} & D_{be} \end{bmatrix} \begin{Bmatrix} T_e - T_\infty \\ 0 \end{Bmatrix} \qquad \text{(eq. 32)}$$

or, expanding back into two individual equations,

$$T_b - T_\infty = A_{be}(T_e - T_\infty) \qquad \text{(eq. 33)}$$

$$Q = C_{be}(T_e - T_\infty) \quad \text{(eq. 34)}$$

Thus, the normalized temperature rise at the adiabatic external board radius is:

$$\frac{T_e - T_\infty}{Q} = \frac{1}{C_{be}} \quad \text{(eq. 35)}$$

and the normalized temperature rise at the inner radius, Ψ_{BA} is:

$$\frac{T_b - T_\infty}{Q} = \frac{A_{be}}{C_{be}} \quad \text{(eq. 36)}$$

For quantitative results, the procedure is to compute the system transmission matrix from the individual domains' **T**'s. From that, extract just the two elements necessary to compute Equation 36. Figure 8 is a plot for three cases of interest, a min−pad board, and a 1−inch copper heat−spreader board with two different thicknesses of copper (1 oz and 2 oz). The horizontal axis is named *package radius*, and is the board inner radius r_b.

A second commonly asked question is, for a given package, how does the thermal performance vary with copper area? Equation 32 again contains the answer, if we now hold the package size as a constant, and vary the intermediate domain boundary, r_s. Though not explicit when we presented Equation 36, this intermediate boundary radius appears in the second half of $\mathbf{T}_{bs}$, and the first half of $\mathbf{T}_{se}$. (In Figure 8, it was a constant corresponding to the "radius" of the 1−inch square pad.) Figure 9 shows a sample of these alternate possibilities arising from Equation 36.

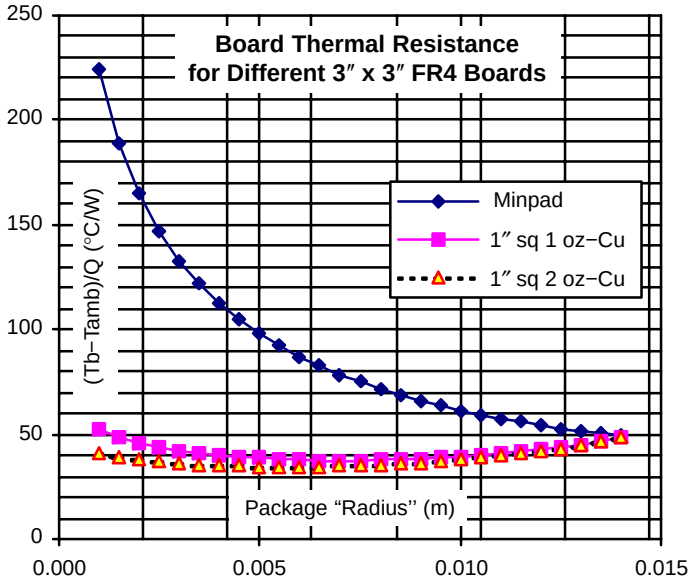

Figure 8. Board Thermal Resistance, Varying Package Size

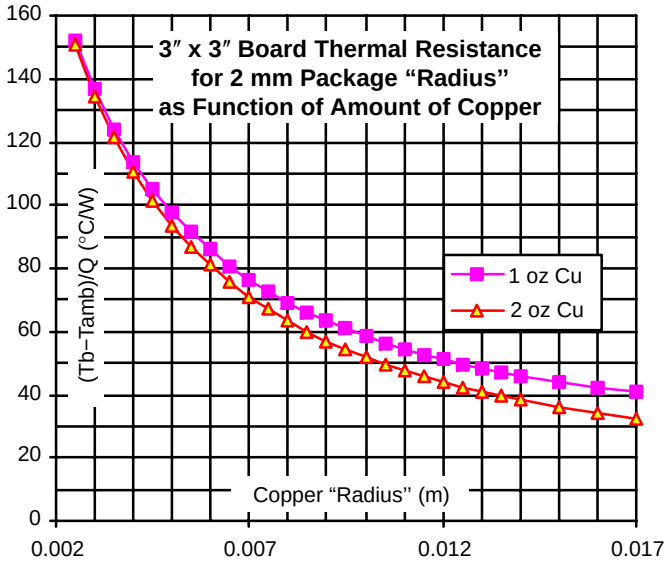

Figure 9. Board Thermal Resistance Varying Copper Size

Solution for Internal Temperature Profile

At the outset, it was suggested that a two−port model was ideally suited for a system−level view of the test board, that is, overall performance without requiring internal solution details. However, the two−port board model in fact can be used to predict the temperature profile within the various zones. (Indeed, this was how Equation 27 is derived in the Appendix.) Specifically, temperature rise as a function of distance from the heat source, is precisely the “interaction strength” that one device (heat source) has on other nearby devices. It mainly depends on the thermal characteristics of the board, and has practically nothing to do with particular package characteristics. Adding even more motivation, the so called “reciprocity theorem” (1,2) allows us to determine the interaction strength of locations in geometries which would otherwise be intractable to analyze directly. For example, the axisymmetric problem in the left of Figure 10 we can solve using the techniques outlined here, whereas to obtain a complete closed−form solution to the one on the right, with an eccentric heat source, is extremely difficult, if not impossible. Yet the reciprocity theorem says that the response at the center of the board to the eccentric heat source, will be identical to the response of the eccentric position to a central heat source.

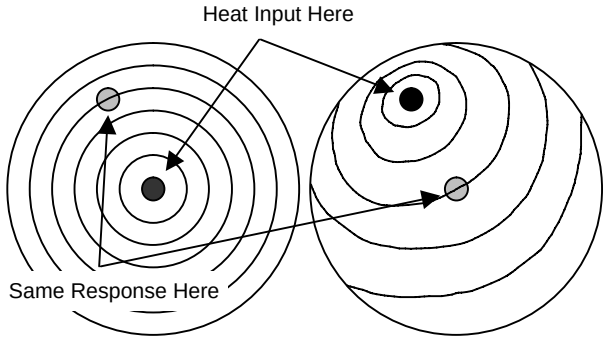

Figure 10. Illustration of the Reciprocity Theorem

To solve for the internal temperature profile in the axisymmetric board model, we note again that any number of two−ports may be cascaded, resulting in but a more complex two−port. It still has but four transmission parameters, though it may be extremely tedious to write them explicitly in symbolic form. With automated computational tools, however, a lengthy string of two−ports is effectively no different than a finite element model. In the case of our axisymmetric board, we could, for instance, model arbitrarily varying convection, conduction, or thickness as a function of radius. To predict the internal temperature profile of our 1−inch pad board, however, it suffices to expand our existing system to use four zones, as illustrated in Figure 11.

How does this help? As we noted earlier in the two−zone model of the 1−inch pad board, when the material properties are the same in the two zones, the model corresponds overall to the min−pad board, or single−zone problem. Clearly, then, if the two zones on either side of a boundary have the same properties, then the specific position of the boundary is irrelevant to the overall behavior of the model (shown rigorously in the Appendix).

On the other hand, if we solve for the potential and flow at the internal boundary, we obtain different values, depending obviously on exactly where the boundary is placed. Thus, a variable radius boundary, within a zone of constant properties, serves as a probe for the temperature and flow within that region. For example, suppose we want the temperature profile within the inner, copper plated region of the 1−inch board model. We construct a new transmission matrix:

$$\mathbf{T}_{r_i e} = \mathbf{T}_{r_i s} \cdot \mathbf{T}_{se} \qquad \text{for } r_b \le r_i \le r_s \quad \text{(eq. 37)}$$

where $\mathbf{T}_{se}$ is exactly as before, but now $\mathbf{T}_{r_i s}$ is based on the 1−inch pad domain properties with a variable inner radius r_i. The following parallel to Equation 32 results:

$$\begin{Bmatrix} T(r_i)-T_\infty \\ q(r_i) \end{Bmatrix} = \begin{bmatrix} A_{r_i e} & B_{r_i e} \\ C_{r_i e} & D_{r_i e} \end{bmatrix} \begin{Bmatrix} T_e-T_\infty \\ 0 \end{Bmatrix} \quad \text{(eq. 38)}$$

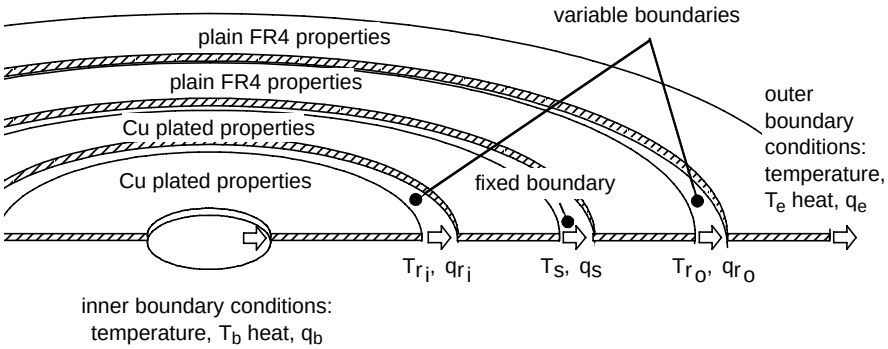

Figure 11. Multiple Regions of Annular Geometry

What we do *not* want now is:

$$\frac{T(r_i)-T_\infty}{q(r_i)} = \frac{A_{rie}}{C_{rie}}$$

because Q, upon which our normalization in Equation 32 is based, is definitely not the same as $q(r_i)$. (The reason is that some of the device power has been dissipated by convection in the area between r_b and the radius we're trying to probe.) Rather, from Equation 38 we obtain:

$$T(r_i)-T_\infty = A_{rie}(T_e-T_\infty) \qquad \text{(eq. 39)}$$

and putting this together with Equation 33, the correct expression is:

$$\frac{T(r_i)-T_\infty}{Q} = \frac{A_{rie}}{C_{be}} \qquad \text{for } r_b \le r_i \le r_s \qquad \text{(eq. 40)}$$

Similarly, we have in the outer region:

$$\frac{T(r_o)-T_\infty}{Q} = \frac{A_{roe}}{C_{be}} \qquad \text{for } r_s \le r_o \le r_e \qquad \text{(eq. 41)}$$

where we find A_{roe} directly from what previously was the $\mathbf{T}_{se}$ transmission matrix, but now evaluated at a variable inner radius r_o, rather than the fixed 1−inch "square" spreader radius r_s. Equations 40 and 41 have been used to generate the results shown in Figure 13 for the same three boards previously analyzed in Figure 8, and two of which were analyzed also in Figure 9. Observe, for example, that the value of 47°C/W appears in all three figures for the specific case of the 1 in−1 oz board at a package (or board inner) radius of 0.002 m. (In Figure 9, this value is found at a copper radius of 0.014 m, which is the circular radius giving an area of 1 sq. in. and was the spreader radius used to generate Figures 8 and 13).

Figure 12 shows a 1−inch−pad thermal test board with an "SMB" body−style package, and eight thermocouples placed at various locations on the board, four TC's along a diagonal from the device to the corner of the board, and four on a line through the center of the package and parallel to the board (and 1−inch pad). TC's were soldered to the pad locations, and glued at the FR4 locations. The SMB has a body size of approximately 0.0033 x 0.0043 m, and its two leads are 0.005 m apart.

For the purposes of Figure 14, the SMB was modeled as a centered, axisymmetric heat source of radius 0.003 m. Ψ_{BA} was calculated for each TC based on total heat dissipation of the device. Measurements were made at both 0.75 W and 1.5 W and averaged for the chart. The only TC reading that does not have excellent agreement with the model is the one at the corner of the 1−inch pad, where its actual distance is apparently larger than its "effective" distance from the heat source. In fact, it is very close to the perimeter of the pad, so it might be that a better measure of "distance" on a square spreader such as this is its relative position as compared to the circularized spreader radius; this would shift it to just left of the pad edge in Figure 14, where it obviously would be in much better agreement with the axisymmetric model.

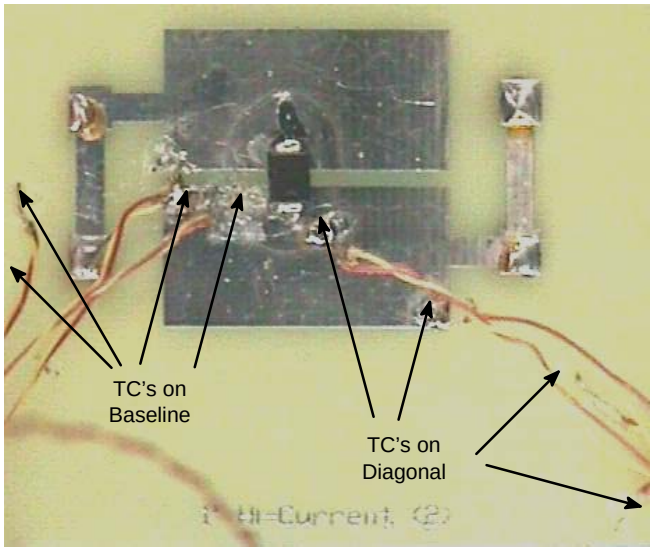

Figure 12. SMB and TC's on 1−inch Pad Thermal Test Board

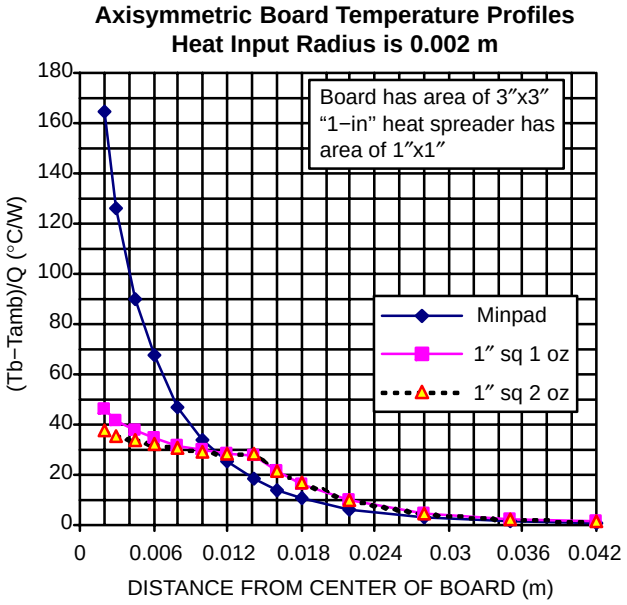

Figure 13. Temperature Profile Over Board Radius

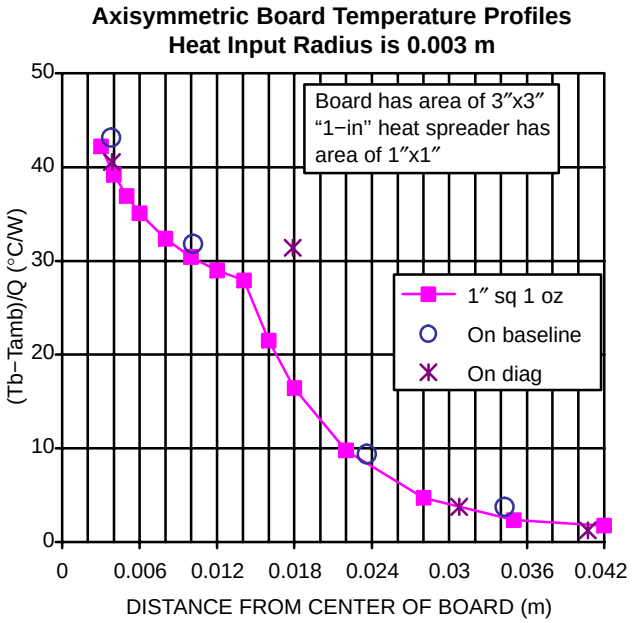

Figure 14. Axisymmetric Board Profile vs. Actual 1″ Pad Data

Limitations

Aside from the obvious limitations of imposing the simplifying axisymmetric assumptions onto far more complicated real geometries, the main limitation not discussed to this point is the assumption that 100% of the device power is deposited into the board at the inner boundary of the axisymmetric model. In reality, of course, some device power will be lost by convection and radiation directly into the ambient environment from the exposed surface of the package; similarly, some will be lost from the (presumably continuous and exposed) far side surface of the board beneath the package (and therefore inside the nominal inner boundary radius). In many cases, this amount of heat loss is a negligible fraction of the total. When it is not, the two−port board model provides the true thermal resistance of the board’s path, facilitating the construction of a more complete model that accounts for these additional heat losses in parallel to it. This would be approach when, for example, the package has a locally applied heatsink that diverts a significant portion of the package power directly into the air above the package, thus bypassing the board. The two−port solution provides the thermal resistance of the board to be modeled as a parallel resistance to the heatsink path.

Final Discussion – Why Bother?

Anyone with a little mathematical knowledge can fit a polynomial curve to the data of Figures 5, 6, 13, or 14. Anyone, even with no mathematical knowledge, but with a modern spreadsheet program, can fit any number of types of curves to the same data. Only a physics based method, however, can provide the correct form of the curve to which that data *should* be fit, and thus with any justification extrapolated beyond the endpoints, or to somewhat different conditions. It is remarkable indeed, and a testimony to the validity of the preceding assertion, that the simple 2D axisymmetric two−port developed in this paper does so well in fitting actual data from real life, 3D non−axisymmetric situations. That it may be implemented in a spreadsheet program with a few simple formulas (see the Appendix), makes it well worth the effort in deriving. All the more so, given that it may be easily extended, using the same simple computational tools, to more complex systems, limitations notwithstanding.

It has been suggested that because one needs a computer to readily implement the axisymmetric thermal two−port, there is little value in utilizing it in preference to a more sophisticated (and therefore less approximate) computerized methodology, for example, a full finite element or finite difference thermal modeler. Unfortunately, many end users of semiconductor packages, especially of the “commodity” type, have no more sophistication than a common spreadsheet program, nor are they willing or able to invest in a more specialized tool. Likewise, manufacturers of commodity semiconductor devices are often asked to provide very simple, quick responses to questions on thermal performance, without sufficient information to accurately define the end application at all. There is a place, therefore, for a modeling method which accounts for the actual physics of a combined convection/conduction thermal system using the most mundane of computer tools, with very little investment in time and detail. It may require the knowledge of a thermal specialist, but it need not require other specialized resources.

SUMMARY AND CONCLUSIONS

A simple axisymmetric board model (the equivalent of a “circular fin”) was used as the foundation for a two−port network thermal analysis. It was shown to match reasonably well certain situations of actual thermal test board data. Multiple two−ports cascaded together enabled complex models of multiple zones of constant property domains to be constructed. This two−port network method was then used to quickly construct parameterized predictions of board−ambient thermal characteristics using the simplest possible idealization of a semiconductor package, that is, a heat source of a certain size. It also was shown that the two−port method may be used to predict temperature gradients within a board. This, in turn, permits rough estimates of component interactions in more complex thermal environments.

ACKNOWLEDGMENTS

The author would like to acknowledge the dedicated efforts of the staff of the ON Semiconductor Thermal Characterization Lab, specifically Ron Lawson, without whom we would have no test equipment with which to perform high quality thermal transient cooling tests, nor data to analyze.

APPENDIX

Modified Bessel's Equation

A particular form of Bessel's equation:

$$\frac{d^2\theta}{dz^2} + \frac{1}{z}\frac{d\theta}{dz} + \left(-1 - \frac{p^2}{z^2}\right)\theta = 0 \qquad \text{(eq. A1)}$$

has as its general solution the modified Bessel functions of the first and second kinds, usually denoted $I_p(z)$ and $K_p(z)$ respectively. Comparison of this equation with the axisymmetric governing Equation 12:

$$\frac{d^2\theta}{dz^2} + \frac{1}{z}\frac{d\theta}{dz} - \theta = 0$$

shows that our problem is the special case where $p = 0$, hence the two linearly independent solutions for our second order problem will be $I_0(z)$ and $K_0(z)$.

The derivatives of the modified Bessel functions are given in general as:

$$\frac{dI_p(az)}{dz} = aI_{p+1}(az) + \frac{p}{z}I_p(az) \qquad \text{(eq. A2)}$$

$$\frac{dK_p(az)}{dz} = -aK_{p+1}(az) + \frac{p}{z}K_p(az) \qquad \text{(eq. A3)}$$

Thus the specific derivatives of our solutions will be:

$$\frac{dI_0(z)}{dz} = I_1(z) \quad \text{and} \quad \frac{dK_0(z)}{dz} = -K_1(z) \qquad \text{(eq. A4)}$$

We thus arrive at the general solutions for potential and flow given in the body of the paper as Equations 13 and 16.

Expansion of Axisymmetric Transmission Matrix

Given the axisymmetric transmission matrix, with $G_i = 2\pi k t z_i$ (see Equation 24):

$$\mathbf{T}_{ij} = \begin{pmatrix} I_0(z_i) & K_0(z_i) \\ -G_i I_1(z_i) & G_i K_1(z_i) \end{pmatrix} \begin{pmatrix} I_0(z_j) & K_0(z_j) \\ -G_j I_1(z_j) & G_j K_1(z_j) \end{pmatrix}^{-1}$$

recall:

$$\det\begin{bmatrix} a & b \\ c & d \end{bmatrix} = ad - bc \quad \text{and} \quad \begin{bmatrix} a & b \\ c & d \end{bmatrix}^{-1} = \frac{1}{ad-bc}\begin{bmatrix} d & -b \\ -c & a \end{bmatrix}$$

thus Equation 24 may be expanded into the more explicit form:

$$\mathbf{T}_{ij} = \frac{\begin{pmatrix} I_1(z_j)K_0(z_i) + I_0(z_i)K_1(z_j) & \frac{I_0(z_j)K_0(z_i) - I_0(z_i)K_0(z_j)}{2\pi k t z_j} \\ 2\pi k t z_i[I_1(z_j)K_1(z_i) - I_1(z_i)K_1(z_j)] & \frac{z_i}{z_j}[I_1(z_i)K_0(z_j) + I_0(z_j)K_1(z_i)] \end{pmatrix}}{I_1(z_j)K_0(z_j) + I_0(z_j)K_1(z_j)} \qquad \text{(eq. A5)}$$

Now the Wronskian of $I_p(z)$ and $K_p(z)$ states (11):

$$I_{p+1}(z)K_p(z) + I_p(z)K_{p+1}(z) = \frac{1}{z} \qquad \text{(eq. A6)}$$

hence Equation A5 becomes, more simply:

$$\mathbf{T}_{ij} = \begin{pmatrix} z_j[I_1(z_j)K_0(z_i) + I_0(z_i)K_1(z_j)] & \frac{I_0(z_j)K_0(z_i) - I_0(z_i)K_0(z_j)}{2\pi k t} \\ 2\pi k t z_j z_i[I_1(z_j)K_1(z_i) - I_1(z_i)K_1(z_j)] & z_i[I_1(z_i)K_0(z_j) + I_0(z_j)K_1(z_i)] \end{pmatrix} \qquad \text{(eq. A7)}$$

Equation A6 also allows us to quickly demonstrate the expected identity for the properly formed two−port:

$$\det \mathbf{T}_{ij} = \frac{z_i[I_1(z_i)K_0(z_i) + I_0(z_i)K_1(z_i)]}{z_j[I_1(z_j)K_0(z_j) + I_0(z_j)K_1(z_j)]} = 1$$

Variable Radius within Constant Property Region

Consider the cascaded transmission matrices based on Equation 24 for two zones, b and e, separated by boundary s.

$$\mathbf{T}_{bs} = \begin{pmatrix} I_0(z_b) & K_0(z_b) \\ -a_1 z_b I_1(z_b) & a_1 z_b K_1(z_b) \end{pmatrix} \begin{pmatrix} I_0(z_s) & K_0(z_s) \\ -a_1 z_s I_1(z_s) & a_1 z_s K_1(z_s) \end{pmatrix}^{-1} \quad \text{(eq. A8)}$$

$$\mathbf{T}_{se} = \begin{pmatrix} I_0(z_s) & K_0(z_s) \\ -a_2 z_s I_1(z_s) & a_2 z_s K_1(z_s) \end{pmatrix} \begin{pmatrix} I_0(z_e) & K_0(z_e) \\ -a_2 z_e I_1(z_e) & a_2 z_e K_1(z_e) \end{pmatrix}^{-1} \quad \text{(eq. A9)}$$

where $a_x = 2\pi k_x t_x$.

The overall transmission matrix $\mathbf{T}_{be}$ is thus:

$$\mathbf{T}_{be} = \begin{pmatrix} I_0(z_b) & K_0(z_b) \\ -a_1 z_b I_1(z_b) & a_1 z_b K_1(z_b) \end{pmatrix} \begin{pmatrix} I_0(z_s) & K_0(z_s) \\ -a_1 z_s I_1(z_s) & a_1 z_s K_1(z_s) \end{pmatrix}^{-1} \cdot \begin{pmatrix} I_0(z_s) & K_0(z_s) \\ -a_2 z_s I_1(z_s) & a_2 z_s K_1(z_s) \end{pmatrix} \begin{pmatrix} I_0(z_e) & K_0(z_e) \\ -a_2 z_e I_1(z_e) & a_2 z_e K_1(z_e) \end{pmatrix}^{-1} \quad \text{(eq. A10)}$$

but if the properties of the two regions are the same, then $a_1 = a_2 = a$, and the two matrices in the center are their own inverses. They thus cancel out, yielding:

$$\mathbf{T}_{be} = \begin{pmatrix} I_0(z_b) & K_0(z_b) \\ -a z_s I_1(z_b) & a z_s K_1(z_b) \end{pmatrix} \begin{pmatrix} I_0(z_e) & K_0(z_e) \\ -a z_e I_1(z_e) & a z_e K_1(z_e) \end{pmatrix}^{-1} \quad \text{(eq. A11)}$$

which is, of course, what we would have had for the entire region b−e having uniform properties in the first place.

Adiabatic Fin Derived from Two−Port Solution

Equation (A7) may be written for the whole domain from b to e, and also for an internal region of variable radius, out to e. Thus:

$$\mathbf{T}_{be} = \begin{pmatrix} z_e[I_1(z_e)K_0(z_b) + I_0(z_b)K_1(z_e)] & \frac{I_0(z_e)K_0(z_b) - I_0(z_b)K_0(z_e)}{2\pi kt} \\ 2\pi kt z_e z_b[I_1(z_e)K_1(z_b) - I_1(z_b)K_1(z_e)] & z_i[I_1(z_b)K_0(z_e) + I_0(z_e)K_1(z_b)] \end{pmatrix} \quad \text{(eq. A12)}$$

$$\mathbf{T}_{re} = \begin{pmatrix} z_e[I_1(z_e)K_0(z) + I_0(z)K_1(z_e)] & \frac{I_0(z_e)K_0(z) - I_0(z)K_0(z_e)}{2\pi kt} \\ 2\pi kt z_e z[I_1(z_e)K_1(z) - I_1(z)K_1(z_e)] & z_i[I_1(z)K_0(z_e) + I_0(z_e)K_1(z)] \end{pmatrix} \quad \text{(eq. A13)}$$

Similarly, applying the adiabatic condition at z_e to (A12) yields, for the temperature equation:

$$T_b - T_\infty = z_e[I_1(z_e)K_0(z_b) + I_0(z_b)K_1(z_e)](T_e - T_\infty) \quad \text{(eq. A14)}$$

and for the flow equation:

$$Q = 2\pi kt z_e z_b[I_1(z_e)K_1(z_b) - I_1(z_b)K_1(z_e)](T_e - T_\infty) \quad \text{(eq. A15)}$$

Applying the adiabatic condition at z_e to (A13) yields:

$$T(z) - T_\infty = z_e[I_1(z_e)K_0(z) + I_0(z)K_1(z_e)](T_e - T_\infty) \quad \text{(eq. A16)}$$

and:

$$q(z) = 2\pi k t z_e z [I_1(z_e)K_1(z) - I_1(z)K_1(z_e)](T_e - T_\infty) \quad \text{(eq. A17)}$$

Now the ratio of (A14) to (A16) yields the conventional adiabatic circular fin relationship between temperature at any radius in terms of the temperature rise at the base of the fin:

$$\frac{T(z)-T_\infty}{T_b-T_\infty} = \frac{z_e[I_1(z_e)K_0(z) + I_0(z)K_1(z_e)](T_e-T_\infty)}{z_e[I_1(z_e)K_0(z_b) + I_0(z_b)K_1(z_e)](T_e-T_\infty)} = \frac{I_1(z_e)K_0(z) + I_0(z)K_1(z_e)}{I_1(z_e)K_0(z_b) + I_0(z_b)K_1(z_e)} \quad \text{(eq. A18)}$$

which, with the change of variable $z_i = mr_i$, was stipulated in the body of the paper as Equation 27.

To put the local temperature rise in terms of device power dissipation, simply divide (A15) into (A16), thus:

$$\frac{T(z)-T_\infty}{Q} = \frac{z_e[I_1(z_e)K_0(z) + I_0(z)K_1(z_e)](T_e-T_\infty)}{2\pi k t z_e z_b[I_1(z_e)K_1(z_b) - I_1(z_b)K_1(z_e)](T_e-T_\infty)} = \frac{1}{2\pi k t z_b}\frac{I_1(z_e)K_0(z) + I_0(z)K_1(z_e)}{I_1(z_e)K_1(z_b) - I_1(z_b)K_1(z_e)} \quad \text{(eq. A19)}$$

constant terms may be collected as follows:

$$\frac{T(z)-T_\infty}{Q} = \frac{1}{2\pi k t z_b}\frac{\frac{I_1(z_e)}{K_1(z_e)}K_0(z) + I_0(z)}{\frac{I_1(z_e)K_1(z_b)}{K_1(z_e)} - I_1(z_b)} = c\left[\frac{I_1(z_e)}{K_1(z_e)}K_0(z) + I_0(z)\right] \quad \text{(eq. A20)}$$

where, also as used in Equation 28 in the main body:

$$c = \frac{1}{2\pi k t z_b}\frac{1}{\frac{I_1(z_e)K_1(z_b)}{K_1(z_e)} - I_1(z_b)} \quad \text{(eq. A21)}$$

Spreadsheet Implementation of Two−Port Model

Perhaps the most universally accessible, computerized mathematical tool is the Microsoft® Excel spreadsheet program. The axisymmetric thermal two−port is easily implemented using simple formulas, as suggested below. Probably the only difficulty the casual Excel user might encounter is that the modified Bessel functions are hidden away in the “Analysis Toolpak,” which takes a (one time only) extra step to access. (Specifically, one goes to the **Tools: Add−Ins** menu, and checks the **Analysis Toolpak** checkbox.) Note that in the following examples, items in uppercase indicate built−in Excel functions.

First, variables may be defined with mnemonic names such as mval1, rad1, etc., according to the region of the board model in question. This obviously facilitates a parametric model, where changes in geometry (board thickness, radii of interest), and thermal properties (convection coefficients, conduction properties, etc.) are built in to these variables’ own formulas.

Second, the symmetry of the transmission matrix, as seen in Equations 24 and 25, lends itself to visually “clean” coding into subgroups of four cells each, each of which is also assigned a mnemonic name, for instance:

Zone 1 Matrix at r1, “Izone1”	
=BESSELI(mval1*rad1,0)	=BESSELK(mval1*rad1,0)
=−cval1*rad1*BESSELI (mval1*rad1,1)	=−cval1*rad1*BESSELK (mval1*rad1,1)

Zone 1 Matrix at r2, “rzone1”	
=BESSELI(mval1*rad2,0)	=BESSELK(mval1*rad2,0)
=−cval1*rad2*BESSELI (mval1*rad2,1)	=−cval1*rad2*BESSELK (mval1*rad2,1)

The Excel formula to create the zone−1 transmission matrix is then:

{=MMULT(lzone1,MINVERSE(rzone1))} (eq. A22)

which must, using normal Excel methods, be properly entered comprising four cells of its own (and presumably with its own mnemonic name, say tzone1). Without going into more detail here, the expression shown as Equation A22 is called an “array formula,” so indicated by the curly braces surrounding the expression. Besides the mnemonic name for the zone−1 transmission matrix, each of its four individual cells might also be named according to its position as one of the four standard transmission parameters, for instance tzone1A, tzone1B, etc.

If several zones are needed for the model (for instance, four zones are needed to compute the graph of Figures 13 and 14), each zone would have its own separate variables and cells defined in exact similarity to that shown above for zone−1. Then, the overall transmission matrix would be computed with another array formula, for instance:

{=MMULT(tzone1,MMULT(tzone2,MMULT(tzone3,tzone4)))} (eq. A23)

If desired for subsequent formulas, as would be needed for Equations 40 and 41 as an overall transmission parameter of the entire system, thus Equation 40 might be represented by:

=tzone4A/tsysC (eq. A24)

REFERENCES

1. H.H. Skilling, Electrical Networks, John Wiley and Sons, 1974.
2. L. Weinberg, Network Analysis and Synthesis, McGraw Hill Book Company, Inc., 1962.
3. E.R.G. Eckert & R.M. Drake Jr., Heat and Mass Transfer, McGraw Hill, 1959.
4. J. VanSant, Conduction Heat Transfer Solutions, Lawrence Livermore National Laboratory, Livermore, CA, 1980.
5. H.S. Carslaw & J.C. Jaeger, Conduction of Heat In Solids, Oxford Press, 1959.
6. J.P. Holman, Heat Transfer, 3rd Ed., McGraw Hill, 1972.
7. H. Wayland, Complex Variables Applied in Science and Engineering, Van Nostrand Reinhold Company.
8. EIA/JEDEC Standard JESD51−2, Integrated Circuits Thermal Test Method Environmental Conditions − Natural Convection (Still Air), Electronic Industries Alliance, December 1995.
9. EIA/JEDEC Standard JESD51−6, Integrated Circuit Thermal Test Method Environmental Conditions − Forced Convection (Moving Air), Electronic Industries Alliance, March 1999.
10. EIA/JEDEC Standard JESD51−8, Integrated Circuit Thermal Test Method Environmental Conditions − Junction−to−Board, Electronic Industries Alliance, October 1999.
11. M. Abramowitz, I. Stegun (eds), Handbook of Mathematical Functions, Dover Publications, Inc., 9th Printing, Dec. 1972.

PUBLICATION ORDERING INFORMATION

LITERATURE FULFILLMENT:
Literature Distribution Center for ON Semiconductor
P.O. Box 61312, Phoenix, Arizona 85082−1312 USA
Phone: 480−829−7710 or 800−344−3860 Toll Free USA/Canada
Fax: 480−829−7709 or 800−344−3867 Toll Free USA/Canada
Email: orderlit@onsemi.com

N. American Technical Support: 800−282−9855 Toll Free USA/Canada

Japan: ON Semiconductor, Japan Customer Focus Center
2−9−1 Kamimeguro, Meguro−ku, Tokyo, Japan 153−0051
Phone: 81−3−5773−3850

ON Semiconductor Website: http://onsemi.com

Order Literature: http://www.onsemi.com/litorder

For additional information, please contact your local Sales Representative.